J Mol Model (2010) 16:863–876
DOI 10.1007/s00894-009-0583-1

ORIGINAL PAPER

# Antioxidant mechanisms of Quercetin and Myricetin in the gas phase and in solution – a comparison and validation of semi-empirical methods

**Gonçalo C. Justino · Abel J. S. C. Vieira**

Received: 31 March 2009 / Accepted: 17 August 2009 / Published online: 25 September 2009


**Abstract** Flavonoids have long been recognized for their general health-promoting properties, of which their antioxidant activity may play an important role. In this work we have studied the properties of two flavonols, quercetin and myricetin, using semi-empirical methods in order to validate the application of the recent Parametric Model 6 and to understand the fundamental difference between the two molecules. Their geometries have been optimized and important molecular properties have been calculated. The energetic of the possible antioxidant mechanisms have also been analyzed. The two studied flavonols do not differ significantly in their molecular properties, but the antioxidant mechanisms by which they may act in solution can be rather different. Moreover, we also show that the Parametric Model 6 can produce reliable information for this type of compounds.

**Keywords** Antioxidant mechanism · Flavonoids · Semi-empirical methods

## Introduction

Flavones and flavonols are two of the most important classes of compounds from the dietary phytochemicals, not only in terms of their greater abundance in the diet, but also due to the recognition of their in vitro antioxidant properties [1–3]. Moreover, several studies have shown that flavonoids contribute to the overall antioxidant capacity in vivo [4, 5]. Besides their antioxidant activity, both flavonoid aglycones and glycosides can act as antifungal, insect antifeedants, antimicrobials and antivirals and *anti*-inflammatory, and are also of particular importance in chemotaxonomy [6–8]. Associated with this, their identification in numerous herbs and infusions has also been the focus of several groups worldwide, particularly from regions where traditional medicine plays an important role [9, 10]. Recently, they have also received considerable interest in the food industry as food additives and as nutraceuticals because of their antioxidant and anticarcinogenic properties, among others [11–14].

Quercetin (3,5,7,3′,4′-penta-hydroxyflavone) is one of the most important flavonoids in diet due to its abundance in foods and to its bioavailability [15], and its antioxidant activity has been well studied [16]. On the other hand, several works have shown that myricetin (3,5,7,3′,4′,5′-hexa-hydroxyflavone) is a stronger antioxidant than quercetin, what has been attributed to the presence of the 5′-OH group that allows a further stabilization of the myricetin derived semi-quinone radical [17, 18]. Briefly, it has been found that myricetin is a stronger brain neuron oxidative stress and liposome oxidation inhibitor than quercetin. Moreover, the pyrogallol moiety present in myricetin is a better superoxide scavenger than the catechol moiety present in quercetin [19]. The structures of these flavonoids are presented in Fig. 1.

Several studies have pointed out the key factors determining the antioxidative potential of a compound, that include i) a low O-H bond dissociation enthalpy (BDE), easing H abstraction; ii) a high ionization potential (IP), hampering oxygen reduction by the antioxidant; and iii) an

**Electronic supplementary material** The online version of this article (doi:10.1007/s00894-009-0583-1) contains supplementary material, which is available to authorized users.

G. C. Justino (✉) · A. J. S. C. Vieira
Requimte/CQFB – Departamento de Química,
Faculdade de Ciências e Tecnologia, Universidade Nova de Lisboa,
2829-516 Caparica, Portugal
e-mail: jgcj@fct.unl.pt

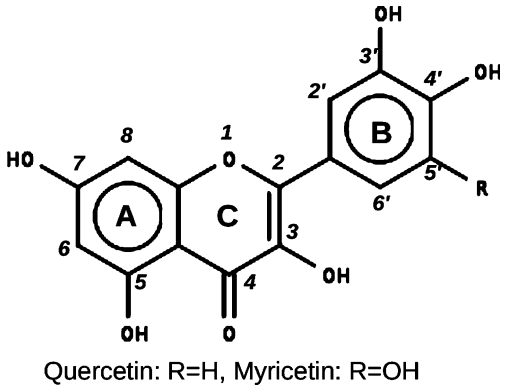


**Fig. 1** Basic structure of quercetin and myricetin. The ring naming and atom numbering are shown

adequate solubility [20]. Moreover, the stability of the antioxidant-derived radicals must also be considered, as unstable radicals may react with other molecules instead of terminating the radical reactions [20].

In this work we present a semi-empirical study, conducted using the PM6 Hamiltonian, in the gas phase and in the water phase, of quercetin, myricetin and their derived radical and anionic species, where we address the above-mentioned pre-requisites of a high antioxidant activity in order to determine which structural and electronic features are behind the higher antioxidant activity of myricetin and to elucidate the role of each of the three possible mechanisms underlying antioxidant activity, namely a) H atom abstraction (HAT), b) sequential proton loss electron transfer (SPLET) and c) single-electron transfer followed by proton transfer (SETPT) [21]; these mechanisms are depicted in Fig. 2.

## Computational details

In the present study, quercetin and myricetin molecules were considered theoretically by performing semi-empirical molecular orbital calculations both in the gas phase and in the water phase. The neutral forms and their anions, the radicals formed by H atom abstraction and the radical cations and radical anions of both flavonols were studied. Pre-optimization was performed under a Dreiding type molecular mechanics force field [22], implemented in the Marvin software and the Calculator plugins [23]. The structures thus obtained were fully optimized using MOPAC2009 version 9.034 [24]. Geometry was optimized using the Baker's Eigenvector Following routine [25]. Geometry was considered to be fully optimized when the gradient norm was less than 0.01. Single point-calculations were then performed to compute the properties of the molecules. All computations were performed using the restricted Hartree-Fock formalism.

The following semi-empirical Hamiltonians, as implemented in MOPAC2009, were used: Modified neglect of differential overlap (MNDO) [26], Austin model 1 (AM1) [27] and the derived Recife model 1 (RM1) [28], and the Parameterized model 3 (PM3) [29] and the new parameterized model 6 (PM6) Hamiltonian [30]. Water phase optimizations and calculations were performed using the Conductor-like Screening Model, a continuum approach to the solvent effect [31]. In order to ensure that the obtained geometries corresponded to absolute energy minimums and not to local ones, quercetin (Q) and myricetin (M) were drawn with dihedral angles (the angle defined by the two planes that contain the B ring and the A and C rings) varying from -180° to 180°in steps of 10° and were subject to geometry optimization. All optimizations converged to the same final structure, as presented hereafter. The dihedral angles obtained for all the computed species with the PM6 Hamiltonian vary between -1.7° and 0.4°. Both these findings are in agreement with previous results that the rotation around the C2-C1′ bond does not constitute a rate limiting step for the antioxidant activity of these compounds due to the low energetic barrier associated with that rotation [32].

The bond dissociation enthalpy (BDE), the proton affinity (PA), the electron transfer enthalpy from the anion (ETE) and the proton dissociation enthalpy from the radical cation (PDE) were calculated as differences between the heats of formation ($H_f$) of the products and the reactants (Fig. 2), where F-O$^{\bullet}$ and F-O$^{-}$ are the radical and the anion derived of the antioxidant, F-OH, respectively. These values allow the analysis of the relevance of each of three proposed mechanisms of antioxidant activity, namely H

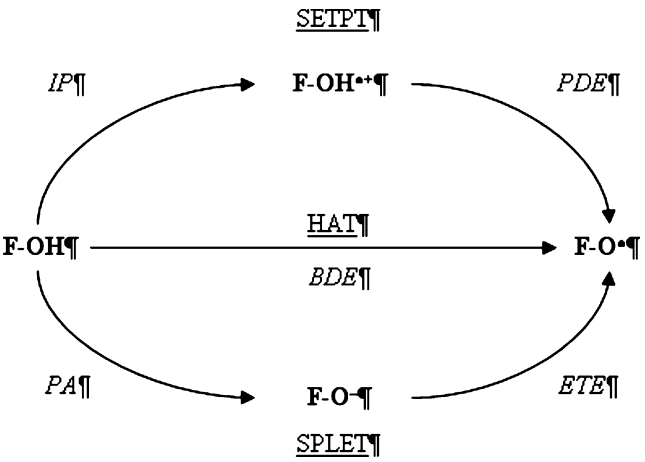


**Fig. 2** Scheme of the analyzed mechanisms of antioxidant activity. SETPT – sequential electron transfer – proton transfer; HAT – H atom abstraction; SPLET – sequential proton loss – electron transfer. IP – ionization potential; PDE – proton dissociation enthalpy; BDE – bond dissociation enthalpy; PA – proton affinity; ETE – electron transfer enthalpy

atom transfer (HAT), quantifiable by the BDE, the single-electron transfer followed by proton transfer (SETPT), quantifiable by the ionization potential and the PDE, and the sequential proton loss electron transfer (SPLET), governed by the proton affinity and ETE [21, 33, 34], as shown in Fig. 2. The heats of formation used for $H^{\bullet}$ and $H^{+}$ were, respectively, 217.99 (which is the actual reference value [35]) and 1303.16 kJ $mol^{-1}$, as calculated with MOPAC2009; although the value for $H^{+}$ differs about 15% from the reference value (1530.17 kJ $mol^{-1}$ [35]), it generates results that are more similar to the DFT results from the literature.

The electronic density-derived properties were computed both from the orbital energies *via* Koopmans' theorem (and denoted with a subscript *O*) and from the total energies (denoted with a subscript *E*) of the species as follows: $IP_E = H_f(FOH^{\bullet+}) - H_f(FOH)$, $IP_O = -E_{HOMO}$, $EA_E = H_f(FOH) - H_f(FOH^{\bullet-})$ and $EA_O = -E_{LUMO}$, where IP and EA stand for ionization potential and electron affinity, respectively. From these, global hardness (η) was computed as $\eta = (IP - EA)/2$, electronegativity (χ) as $\chi = (IP + EA)/2$ and electrophilicity (ω) as $\omega = \chi^2/8\,\eta$ [36, 37]. The energy difference between the LUMO and the HOMO was also computed using the orbital energies, as $\varepsilon_{G,O} = E_{LUMO} - E_{HOMO}$, and using the energetic values for electron affinities and ionization potentials, using $\varepsilon_{G,E} = IP_E - EA_E$.

## Results and discussion

### Comparison of the performance of the different Hamiltonians

Table 1 lists the heats of formation computed using the PM6 Hamiltonians for quercetin and myricetin and their derived radicals and anions; results obtained with the other semi-empirical methods are presented as Supplementary Information. All methods indicate that the most acidic hydroxyl group is the 4′ in both the gas phase and the water phase, and that the H atom more easily abstracted from quercetin is also the 4′ in the gas phase and, in the water phase, either the 3′ or the 4′, though, except in the case of the AM1 method, always with very close heats of formation (with differences inferior to 1 kJ $mol^{-1}$).

In the case of myricetin, the results with the MNDO, AM1 and RM1 methods show a high dispersion of values for the gas phase radicals and for the water phase anions. On the other hand, and considering the structure of myricetin, the most easily abstractable H atom appears to be the 4′ one as the resulting radical is more efficiently stabilized due to the presence of the two neighboring OH groups. However, the mentioned methods indicate that the H atom to be firstly abstracted is the 3 one.

**Table 1** Heats of formation (in kJ $mol^{-1}$) of quercetin (Q) and myricetin (M) and their derived radicals and anions obtained with the PM6 model. $\Delta_{solv}H_f$ values were calculated as $H_f(X_w)$-$H_f(X_g)$

| | $H_fQ$ (g) | $H_fM$ (g) |
|---|---|---|
| F-OH | -975.55 | -1152.72 |
| 3-$O^-$ | -1184.55 | -1377.35 |
| 5-$O^-$ | -1177.00 | -1362.39 |
| 7-$O^-$ | -1216.78 | -1401.10 |
| 3′-$O^-$ | -1129.74 | -1361.34 |
| 4′-$O^-$ | -1212.07 | -1364.81 |
| 5′-$O^-$ | – | -1321.53 |
| F-$OH^{\bullet+}$ | -191.37 | -362.05 |
| 3-$O^{\bullet}$ | -840.13 | -1014.73 |
| 5-$O^{\bullet}$ | -748.52 | -926.37 |
| 7-$O^{\bullet}$ | -768.88 | -944.49 |
| 3′-$O^{\bullet}$ | -834.88 | -1026.54 |
| 4′-$O^{\bullet}$ | -856.93 | -1025.04 |
| 5′-$O^{\bullet}$ | – | -1014.32 |
| | $H_fQ$ (w) | $H_fM$ (w) |
| F-OH | -1052.69 | -1235.44 |
| 3-$O^-$ | -1464.84 | -1659.08 |
| 5-$O^-$ | -1452.84 | -1662.03 |
| 7-$O^-$ | -1486.41 | -1664.08 |
| 3′-$O^-$ | -1448.18 | -1650.27 |
| 4′-$O^-$ | -1468.29 | -1642.41 |
| 5′-$O^-$ | – | -1641.17 |
| F-$OH^{\bullet+}$ | -431.44 | -611.14 |
| 3-$O^{\bullet}$ | -924.67 | -1104.30 |
| 5-$O^{\bullet}$ | -852.88 | -1022.98 |
| 7-$O^{\bullet}$ | -865.09 | -1028.66 |
| 3′-$O^{\bullet}$ | -924.98 | -1106.94 |
| 4′-$O^{\bullet}$ | -928.46 | -1100.94 |
| 5′-$O^{\bullet}$ | – | -1111.62 |
| | $\Delta_{solv}H_fQ$ | $\Delta_{solv}H_fM$ |
| F-OH | -77.14 | -82.72 |
| 3-$O^-$ | -280.29 | -281.73 |
| 5-$O^-$ | -275.84 | -299.64 |
| 7-$O^-$ | -269.63 | -262.97 |
| 3′-$O^-$ | -318.43 | -288.93 |
| 4′-$O^-$ | -256.22 | -277.61 |
| 5′-$O^-$ | – | -319.64 |
| F-$OH^{\bullet+}$ | -240.06 | -249.09 |
| 3-$O^{\bullet}$ | -84.54 | -89.57 |
| 5-$O^{\bullet}$ | -104.36 | -96.62 |
| 7-$O^{\bullet}$ | -96.21 | -84.18 |
| 3′-$O^{\bullet}$ | -90.10 | -80.40 |
| 4′-$O^{\bullet}$ | -71.53 | -75.90 |
| 5′-$O^{\bullet}$ | – | -97.30 |

Results published in the literature [33, 37–44] using several methods (ranging from the semi-empirical AM1 to DFT methods with a 6-311++G(3df,2p) basis, which are presented as Supplementary Information) indicate that the most acidic OH group in quercetin is the 4′ one and that the first H abstraction occurs from the 3-, 3′- or 4′-OH groups, and this variation does not appear to be method-dependent, although the 4′ tends to predominate over gas phase studies and the 3-OH over the water phase studies. For myricetin, the few published results indicate that the 4′-OH group is the most acidic one in both phases. Given these results, we consider that the semi-empirical description of these two flavonoids obtained with the PM6 method, and partially with the PM3 method, is in broad agreement with what has been published so far. Moreover, the results obtained are in agreement with what is expected from the structure of these flavonoids as both the radical and the anion formed from the 4′-OH group are the ones expected to be more stabilized by charge delocalization and resonance.

## Geometry and molecular properties

The closed formulas of quercetin and myricetin are, respectively, $C_{15}H_{10}O_7$ and $C_{15}H_{10}O_8$. The optimized structures of myricetin in the gas and water phases are presented in Fig. 3. The dihedral angles O1C2C1′C2′, formed between the plane containing the A and C rings and the plane containing the B ring, are close to zero, showing that both these molecules are very close to being fully planar. The X-ray structure of crystalline quercetin shows that the angle between the two planes is about 7º [45]. Other works at the RHF level with STO-3G basis set [46] and with the semi-empirical PM3 method [38] have found that quercetin is planar; on the other hand, a work using the semi-empirical MNDO method has found it to be non-planar [47]. Leopoldini et al. [41] calculations at the DFT level, using the B3LYP hybrid functional with the 6-311++G** basis set, have found that quercetin and myricetin are both planar, and also that the 4′ anion of myricetin and all the quercetin anions are planar, thus allowing charge delocalization, with the concomitant enhancement of their antioxidant activity.

Quercetin and myricetin, being constituted of an hydrophobic part, the phenyl rings, and an hydrophilic part, the hydroxylic groups, display an amphipathic behavior. The negative energies of solvation ($\Delta_{solv}H_f$, Table 1) indicate that these flavonoids are soluble, although sparingly, in water; the derived radicals are also water soluble, which is of extreme importance as most of the reactions in which flavonoids participate occur in water or at water/lipid interfaces [48]. Moreover, the computed permanent dipole moments ($\mu_0$, Table 2) also indicate that both Q and M are relatively polarized systems, reflecting the polarized hydroxyl and carbonyl functions present in the structures and corroborating their water solubility.

The total dipole moment due to the presence of external fields is dependent on, besides $\mu_0$, the polarizability $\alpha$ and

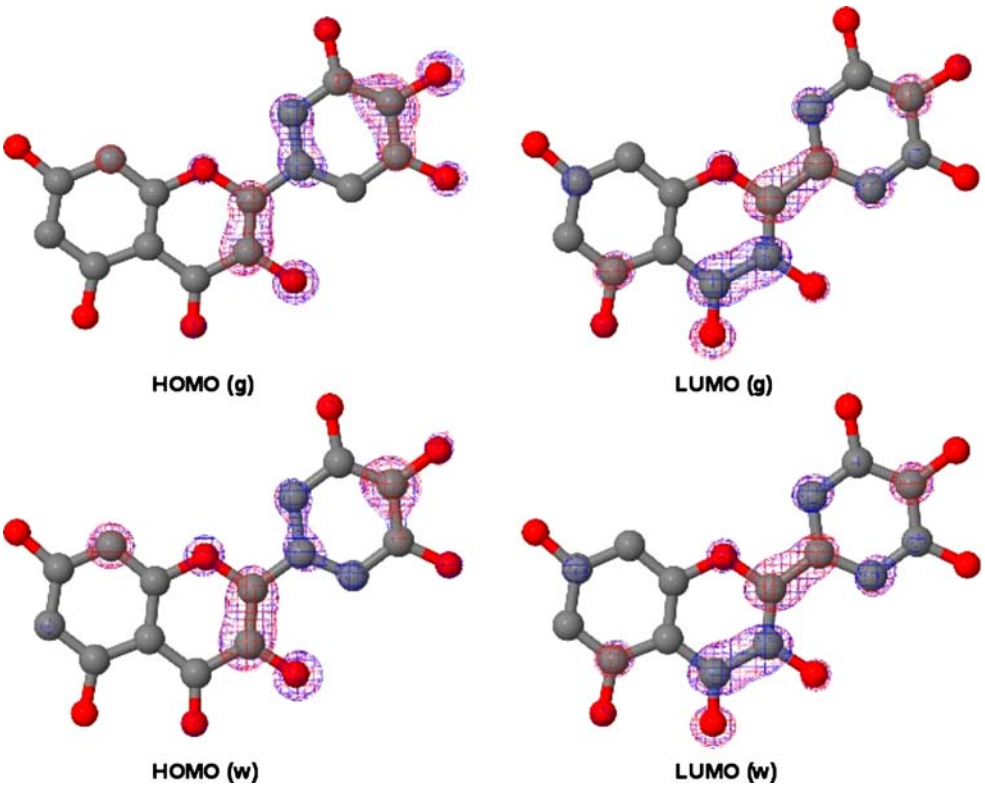


**Fig. 3** Optimized gas phase and water phase structures of myricetin using the semi-empirical PM6 method with superimposed HOMO and LUMO molecular orbitals

**Table 2** Computed properties for the quercetin (Q) and myricetin (M) neutral molecules in the gas and water phases obtained with the PM6 model; IP – ionization potential (in kJ $mol^{-1}$); EA – electron affinity (in kJ $mol^{-1}$); $\chi$ – electronegativity; $\varepsilon_G$ – energy gap between the highest occupied (HOMO) and lowest unoccupied (LUMO) molecular orbitals (in eV); $\eta$ – molecular (or Parr and Pople absolute) hardness (in eV) ; $\omega$ – molecular electrophilicity (in eV); $\mu_0$ – permanent dipole moment (in Debye). Where available, literature data are included for comparison. The *E* and *O* indexes refer to data computed using an energy approach or an orbital approach, respectively. A – data taken from reference 54, obtained at the B3LYP/6-31G(d, p) level; B – data taken from reference 37, using the CHIHDFT method with a CBSB4 basis set

| | $IP_O$ | $IP_E$ | $EA_O$ | $EA_E$ | $\chi_O$ | $\chi_E$ | $\varepsilon_{G,O}$ | $\varepsilon_{G,E}$ | $\eta_O$ | $\eta_E$ | $\omega_O$ | $\omega_E$ | $\mu_0$ |
|---|---|---|---|---|---|---|---|---|---|---|---|---|---|
| M (g) | 854.11 | 790.67 | 140.58 | 69.11 | 5.15 | 4.46 | 7.40 ($3.74^A$) | 7.47 | 3.70 | 3.74 | 0.90 | 0.66 | 3.97 ($1.70^A$) |
| M (w) | 872.83 | 624.30 | 157.28 | 137.25 | 5.34 | 3.95 | 7.42 | 5.05 | 3.71 | 2.52 | 0.96 | 0.77 | 6.35 |
| Q (g) | 848.90 | 784.17 | 129.39 | 165.86 | 5.07 | 4.92 | 7.46 ($3.75^A$) | 6.41 | 3.73 | 3.20 | 0.86 | 0.95 | 4.02 ($2.41^A$) |
| Q (w) | 863.95 ($549.03^B$) | 621.25 ($696.66^B$) | 147.82 ($73.33^B$) | 396.98 ($222.89^B$) | 5.24 ($4.00^B$) | 5.28 ($3.99^B$) | 7.42 | 2.32 | 3.71 ($3.23^B$) | 1.16 ($1.69^B$) | 0.93 ($2.47^B$) | 2.99 ($4.72^B$) | 6.56 |

the first and second order hyperpolarizabilities, $\beta$ and $\gamma$. The values obtained for Q and M, in water, are $\alpha_M$= 229.14 a.u., $\beta_M$=1606.44 a.u., $\gamma_M$=123548.86 a.u., and $\alpha_Q$=225.03 a.u., $\beta_Q$=1868.56 a.u., $\gamma_Q$=125047.11 a.u., and indicate that these flavonoids are capable of polarizing other atoms or molecules and of accommodating themselves to the surrounding environment, indicating that they will be available to interact with surrounding radicals and other species [49, 50]. However, the direction of the dipole varies strongly from species to species, thus it cannot be used as a descriptor of the activity of these compounds.

The high reactivity of these compounds is also characterized by a small energy gap, $\varepsilon_G$, between the HOMO and the LUMO and also by a low LUMO energy, that indicates that these compounds can behave as soft electrophiles [51–53]. The $\varepsilon_G$ values obtained for Q and M are similar, indicating that their reactivity does not differ much. This similar reactivity has also been obtained by DFT computations [54] but the absolute values we obtained are roughly the double of the DFT ones. However, it must be noted that the energy derived $\varepsilon_G$ values in water are, as expected, much smaller than those in the gas phase, a trend that is not observed with $\varepsilon_{G,O}$ values.

The ionization potentials and electron affinities of both Q and M have been computed both from the total energies and from the orbital energies (using Koopman's theorem). The results presented in Table 2 show that while all the values computed with the PM6 orbital values are substantially different than those obtained with a CHIH-DFT method, with differences ranging from 10% to more than twice the DFT value, the PM6 values computed using the energies of the species involved in the processes (the neutral form and the radical cation and anion), the obtained values are in the same range of the values computed at the DFT level. Also, the obtained values also indicate that it is easier for these compounds to yield an electron than to acquire one, thus favoring their action as antioxidants (by reducing other species) than as putative pro-oxidants (by oxidizing other species).

A higher hardness index ($\eta$) is associated with a lower reactivity, and the results in Table 2 indicate that the energy-derived hardnesses of Q and M are lower in water than in the gas phase, thus suggesting a higher reactivity in the condensed phase, as expected from a lower ionization potential in water than in the gas phase, or in other words, a higher ability to provide an electron when in the gas phase.

The higher electron affinities of Q and M in water than in the gas phase also indicate that these compounds are more reactive in the condensed phase, where they have a higher ability to accommodate electrons from the solvent of other species (as expected from their higher electrophilicity).

However, the nucleophilic and electrophilic delocalizabilities, presented in Table 3, indicate that the reactivity of the two flavonoids, in terms of the most likely sites of electrophilic and nucleophilic attack, presents a striking difference: while myricetin is most likely to be attacked by electrophiles on the O atoms of the B ring OH groups (where Dn(*r*) hits its maximum values), quercetin is more likely to be attacked by electrophiles on hydroxylic O atoms of the A or C rings. On the other hand, the De(***r***) distribution is similar for both flavonoids in either phase.

In general, energy-derived properties present values that are more similar to their DFT analogues than orbital-derived properties. The best example is the ionization potential of Q and M. Also, the variations of the electron-derived properties, when comparing the gas phase and the water phases, are also more coherent with what is expected from the point of organic structure and reactivity and are also coherent with their DFT counterparts.

The IP and EA values of $\alpha$-tocopherol, a powerful antioxidant ubiquitous in mammal organisms, were also calculated using the PM6 method. In the water phase, the IP for tocopherol is 539.37 kJ $mol^{-1}$ and the EA is

**Table 3** Nucleophilic – Dn(*r*) – and electrophilic – Dn(*r*) – delocalizabilities of the neutral quercetin (Q) and myricetin (M) molecules in the gas and water phases obtained with the PM6 model

| | M (g) | | M (w) | | Q (g) | | Q (w) | |
|---|---|---|---|---|---|---|---|---|
| | Dn(r) | De(r) | Dn(r) | De(r) | Dn(r) | De(r) | Dn(r) | De(r) |
| O1 | -0.27 | -0.52 | -0.26 | -0.53 | -0.26 | -0.52 | -0.26 | -0.52 |
| C2 | -0.63 | -0.36 | -0.62 | -0.36 | -0.63 | -0.35 | -0.64 | -0.34 |
| C3 | -0.58 | -0.39 | -0.57 | -0.39 | -0.57 | -0.39 | -0.56 | -0.40 |
| O3 | -0.21 | -0.60 | -0.20 | -0.60 | -0.21 | -0.60 | -0.20 | -0.60 |
| C4 | -0.67 | -0.25 | -0.66 | -0.25 | -0.66 | -0.25 | -0.67 | -0.24 |
| O4 | -0.21 | -0.64 | -0.20 | -0.65 | -0.21 | -0.64 | -0.20 | -0.64 |
| C4/C5 | -0.44 | -0.48 | -0.43 | -0.49 | -0.44 | -0.48 | -0.44 | -0.48 |
| C5 | -0.66 | -0.26 | -0.65 | -0.27 | -0.66 | -0.26 | -0.66 | -0.26 |
| O5 | -0.21 | -0.56 | -0.20 | -0.57 | -0.21 | -0.56 | -0.20 | -0.56 |
| C6 | -0.41 | -0.50 | -0.40 | -0.51 | -0.41 | -0.50 | -0.40 | -0.51 |
| C7 | -0.66 | -0.27 | -0.64 | -0.27 | -0.66 | -0.27 | -0.64 | -0.27 |
| O7 | -0.21 | -0.55 | -0.20 | -0.57 | -0.21 | -0.55 | -0.20 | -0.56 |
| C8 | -0.42 | -0.49 | -0.41 | -0.50 | -0.42 | -0.49 | -0.41 | -0.50 |
| C8/O1 | -0.67 | -0.28 | -0.66 | -0.28 | -0.67 | -0.28 | -0.67 | -0.28 |
| C1′ | -0.54 | -0.38 | -0.54 | -0.38 | -0.51 | -0.40 | -0.51 | -0.41 |
| C2′ | -0.46 | -0.47 | -0.46 | -0.47 | -0.48 | -0.44 | -0.48 | -0.43 |
| C3′ | -0.58 | -0.34 | -0.58 | -0.34 | -0.56 | -0.36 | -0.56 | -0.36 |
| O3′ | -0.20 | -0.60 | -0.19 | -0.60 | -0.19 | -0.61 | -0.19 | -0.61 |
| C4′ | -0.55 | -0.41 | -0.54 | -0.41 | -0.58 | -0.37 | -0.58 | -0.36 |
| O4′ | -0.19 | -0.61 | -0.19 | -0.62 | -0.20 | -0.58 | -0.19 | -0.60 |
| C5′ | -0.58 | -0.34 | -0.58 | -0.34 | -0.47 | -0.43 | -0.46 | -0.44 |
| O5′ | -0.20 | -0.58 | -0.19 | -0.60 | - | - | - | - |
| C6′ | -0.46 | -0.47 | -0.45 | -0.47 | -0.49 | -0.43 | -0.49 | -0.42 |

260.68 kJ mol$^{-1}$. In the gas phase, the calculated values are 684.26 and 26.44 kJ mol$^{-1}$, respectively.

The water phase ionization potential of tocopherol is smaller than the corresponding ones of Q and M, indicating that the two flavonoids are able to get an electron from tocopherol. This agrees with the role of flavonoid on the transference of "radical character" from highly oxidant reactive species to antioxidants like tocopherol (and also ascorbate) that are regenerated from the diet (or, in the case of ascorbate, enzymatically) [55].

## Charge and spin delocalization

It is commonly mentioned throughout the literature that planarity is important to the antioxidant activity of flavonoids because it allows charge (in the case of anions) or spin (in the case of radicals) delocalization over the entire molecule, thus contributing to the stabilization of these species. However, as it can be seen in Table 4, and in agreement with other results obtained at the DFT level by Fiorucci et al. [33], charge delocalization is restricted to the ring from where the proton is abstracted and the C ring – when deprotonation occurs from the B ring the resulting atomic charges are mainly located on B and C ring atoms, and when deprotonation occurs from the A ring atomic charges are mainly located on the A and C ring atoms. This effect is more evident in the water phase results than in the gas phase results.

Noticeably, the atomic charge of O atoms does not vary considerably between the neutral form and the anionic forms, and the excess charge is distributed mainly over the rings.

In the case of spin distribution (Table 5), spin accumulates essentially on the ring from where the H atom was abstracted, with only a small percentage of it being located on the central ring. The remarkable exception to this is the case of 3-O$^{\bullet}$ radicals, where spin is also distributed throughout the B ring, which agrees with some published results that indicate that the 3-OH group of quercetin can be particularly important in the antioxidant activity of this flavonoid [40, 56].

It must be noted that the position of the OH group from where abstraction occurs is important – abstraction from the 4′-OH group (which is *para* to the attachment position of the C ring) leads to a higher spin delocalization to the C ring than when it occurs from the 3′ or 5′-OH groups (which are *ortho* to that position). This higher spin delocalization agrees with the abstraction order, where the 4′-OH H atom is the more prone to be removed. Charge

**Table 4** Sum of atomic charges for rings A ($\Sigma q_A$), B ($\Sigma q_B$) and C ($\Sigma q_C$) and for the ring groups AC ($\Sigma q_{AC}$) and BC ($\Sigma q_{BC}$) computed for neutral quercetin and myricetin molecules in the gas and water phases using the PM6 model

| | | Myricetin | | | | | Quercetin | | | | |
|---|---|---|---|---|---|---|---|---|---|---|---|
| | | $\Sigma q_A$ | $\Sigma q_B$ | $\Sigma q_C$ | $\Sigma q_{AC}$ | $\Sigma q_{BC}$ | $\Sigma q_A$ | $\Sigma q_B$ | $\Sigma q_C$ | $\Sigma q_{AC}$ | $\Sigma q_{BC}$ |
| Gas phase | F-OH | 0.18 | 0.09 | −0.27 | −0.09 | −0.18 | 0.18 | 0.09 | −0.27 | −0.09 | −0.18 |
| | 3-O$^-$ | −0.06 | −0.10 | −0.84 | −0.90 | −0.94 | −0.06 | −0.08 | −0.86 | −0.92 | −0.94 |
| | 5-O$^-$ | −0.58 | −0.01 | −0.42 | −1.00 | −0.43 | −1.14 | −0.21 | 0.36 | −0.78 | 0.15 |
| | 7-O$^-$ | −0.50 | 0.01 | −0.51 | −1.01 | −0.50 | −0.51 | 0.02 | −0.51 | −1.02 | −0.49 |
| | 3′-O$^-$ | 0.08 | −0.78 | −0.31 | −0.22 | −1.08 | 0.06 | −0.75 | −0.31 | −0.25 | −1.06 |
| | 4′-O$^-$ | 0.02 | −0.60 | −0.42 | −0.40 | −1.02 | 0.03 | −0.62 | −0.41 | −0.38 | −1.03 |
| | 5′-O$^-$ | 0.07 | −0.77 | −0.30 | −0.23 | −1.07 | | | | | |
| | F-OH$^{\bullet+}$ | 0.36 | 0.67 | −0.03 | 0.33 | 0.64 | 0.39 | 0.38 | 0.03 | 0.43 | 0.42 |
| | 3-O$^\bullet$ | 0.19 | 0.17 | −0.36 | −0.17 | −0.19 | 0.18 | 0.18 | −0.36 | −0.18 | −0.18 |
| | 5-O$^\bullet$ | 0.08 | 0.09 | −0.17 | −0.09 | −0.08 | −0.38 | −0.11 | 0.49 | 0.11 | 0.38 |
| | 7-O$^\bullet$ | 0.08 | 0.11 | −0.19 | −0.11 | −0.08 | 0.07 | 0.12 | −0.19 | −0.12 | −0.07 |
| | 3′-O$^\bullet$ | 0.20 | 0.07 | −0.27 | −0.07 | −0.20 | 0.19 | 0.08 | −0.27 | −0.08 | −0.19 |
| | 4′-O$^\bullet$ | 0.19 | 0.08 | −0.27 | −0.08 | −0.19 | 0.19 | 0.07 | −0.27 | −0.07 | −0.19 |
| | 5′-O$^\bullet$ | 0.19 | 0.08 | −0.27 | −0.08 | −0.19 | | | | | |
| Water phase | F-OH | 0.22 | 0.10 | −0.32 | −0.10 | −0.22 | 0.20 | 0.09 | −0.33 | −0.13 | −0.24 |
| | 5′-O$^-$ | 0.10 | −0.03 | −1.07 | −0.97 | −1.10 | 0.09 | 0.00 | −1.09 | −1.00 | −1.09 |
| | 4′-O$^-$ | −0.63 | 0.06 | −0.43 | −1.06 | −0.37 | −0.63 | 0.07 | −0.45 | −1.07 | −0.37 |
| | 3′-O$^-$ | −0.64 | 0.07 | −0.43 | −1.07 | −0.36 | −0.65 | 0.08 | −0.43 | −1.08 | −0.35 |
| | 7-O$^-$ | 0.20 | −0.87 | −0.33 | −0.13 | −1.20 | 0.20 | −0.86 | −0.34 | −0.14 | −1.20 |
| | 5-O$^-$ | 0.19 | −0.83 | −0.35 | −0.17 | −1.19 | 0.18 | −0.81 | −0.37 | −0.19 | −1.18 |
| | 3-O$^-$ | 0.20 | −0.87 | −0.33 | −0.13 | −1.20 | | | | | |
| | F-OH$^{\bullet+}$ | 0.24 | 0.95 | −0.20 | 0.05 | 0.76 | 0.25 | 0.96 | −0.20 | 0.05 | 0.76 |
| | 5′-O$^\bullet$ | 0.22 | 0.06 | −0.28 | −0.06 | −0.22 | 0.23 | 0.27 | −0.50 | −0.27 | −0.23 |
| | 4′-O$^\bullet$ | 0.22 | 0.05 | −0.27 | −0.05 | −0.22 | −0.51 | 0.61 | −0.10 | −0.61 | 0.51 |
| | 3′-O$^\bullet$ | 0.22 | 0.06 | −0.28 | −0.06 | −0.22 | −0.60 | 0.92 | −0.32 | −0.92 | 0.60 |
| | 7-O$^\bullet$ | −0.58 | 0.9 | −0.32 | −0.9 | 0.58 | 0.22 | 0.07 | −0.28 | −0.07 | −0.22 |
| | 5-O$^\bullet$ | −0.57 | 0.87 | −0.3 | −0.87 | 0.57 | 0.22 | 0.06 | −0.28 | −0.06 | −0.22 |
| | 3-O$^\bullet$ | 0.26 | 0.14 | −0.41 | −0.14 | −0.27 | | | | | |

delocalization to the C ring is also more prominent in the case of the 4′-O$^-$ anions.

All the above discussed characteristics are in agreement with the HOMO and LUMO distribution of quercetin [38] and myricetin (presented in Fig. 3). The HOMO orbitals are mainly disposed on the C2–C3 double bond, the 3-OH group and the B ring, in good agreement with the many experimental results that sustain the importance of those characteristics as key determinants of the flavonoids antioxidant activity (reviewed by Bors and Michel [3]).

## Energetics of the antioxidant processes

Flavonoids have been studied as antioxidants due to the ease with which a H atom can be abstracted from them by a radical, producing a flavonoid radical (F-O$^\bullet$) that is more stable and less reactive than the original attacking radical. The HAT mechanism is primarily governed by the O-H bond dissociation enthalpy (BDE, the energy associated with the homolysis of a hydroxylic O-H bond). More recently, other mechanisms have been described that could be important for the formation of the flavonoid derived radicals, particularly the sequential proton loss electron transfer (SPLET) mechanism and the sequential electron transfer proton transfer (SETPT) mechanism [21, 33, 34].

The SPLET mechanism is expected to be relevant in proton-accepting solvents, as is water, and involves deprotonation of the flavonoid (measurable by proton affinity, PA) followed by electron transfer (measured by the electron transfer enthalpy, ETE) to produce the flavonoid radical. Oppositely, the SETPT mechanism involves formation of the flavonoid radical cation by electron loss from the neutral flavonoid (where the ionization potential, IP, becomes important) followed by deprotonation of the

**Table 5** Sum of spin densities for rings A ($\Sigma s_A$), B ($\Sigma s_B$) and C ($\Sigma s_C$) and for the ring groups AC ($\Sigma s_{AC}$) and BC ($\Sigma s_{BC}$) computed for neutral quercetin and myricetin molecules in the gas and water phases using the PM6 model

| | | Myricetin | | | | | Quercetin | | | | |
|---|---|---|---|---|---|---|---|---|---|---|---|
| | | $\Sigma s_A$ | $\Sigma s_B$ | $\Sigma s_C$ | $\Sigma s_{AC}$ | $\Sigma s_{BC}$ | $\Sigma s_A$ | $\Sigma s_B$ | $\Sigma s_C$ | $\Sigma s_{AC}$ | $\Sigma s_{BC}$ |
| Gas phase | F-OH$^{\bullet+}$ | 0,03 | 0,65 | 0,33 | 0,35 | 0,97 | 0,04 | 0,51 | 0,45 | 0,49 | 0,96 |
| | 3-O$^{\bullet}$ | 0,05 | 0,30 | 0,65 | 0,70 | 0,95 | 0,04 | 0,30 | 0,65 | 0,70 | 0,96 |
| | 5-O$^{\bullet}$ | 0,86 | 0,01 | 0,13 | 0,99 | 0,14 | 0,86 | 0,01 | 0,13 | 0,99 | 0,14 |
| | 7-O$^{\bullet}$ | 0,97 | 0,00 | 0,03 | 1,00 | 0,03 | 0,97 | 0,00 | 0,03 | 1,00 | 0,03 |
| | 3′-O$^{\bullet}$ | 0,00 | 0,98 | 0,02 | 0,02 | 1,00 | 0,00 | 0,98 | 0,01 | 0,02 | 1,00 |
| | 4′-O$^{\bullet}$ | 0,00 | 0,88 | 0,12 | 0,12 | 1,00 | 0,00 | 0,98 | 0,02 | 0,02 | 1,00 |
| | 5′-O$^{\bullet}$ | 0,00 | 0,99 | 0,01 | 0,01 | 1,00 | | | | | |
| Water phase | F-OH$^{\bullet+}$ | 0,00 | 0,89 | 0,10 | 0,11 | 1,00 | 0,00 | 0,89 | 0,11 | 0,11 | 1,00 |
| | 5′-O$^{\bullet}$ | 0,05 | 0,29 | 0,66 | 0,71 | 0,95 | 0,04 | 0,34 | 0,62 | 0,66 | 0,96 |
| | 4′-O$^{\bullet}$ | 0,08 | 0,28 | 0,64 | 0,72 | 0,92 | 0,03 | 0,56 | 0,41 | 0,44 | 0,97 |
| | 3′-O$^{\bullet}$ | 0,08 | 0,27 | 0,65 | 0,73 | 0,92 | 0,01 | 0,86 | 0,13 | 0,14 | 0,99 |
| | 7-O$^{\bullet}$ | 0,00 | 0,97 | 0,03 | 0,03 | 1,00 | 0,00 | 0,97 | 0,03 | 0,03 | 1,00 |
| | 5-O$^{\bullet}$ | 0,00 | 0,89 | 0,11 | 0,11 | 1,00 | 0,00 | 0,97 | 0,03 | 0,03 | 1,00 |
| | 3-O$^{\bullet}$ | 0,00 | 0,98 | 0,02 | 0,02 | 1,00 | | | | | |

radical cation (describable by the proton dissociation enthalpy, PDE). The values computed for these reactions are presented in Table 6 for myricetin and Table 7 for quercetin. Table 8 summarized the orders of deprotonation and H atom abstraction for these compounds obtained with this study and also from published data from other authors.

## Comparison of PM6 and DFT values

In the case of myricetin, the computed PA's were compared with the acidities calculated at various DFT levels [41, 56], and the results differ at most 10% in the gas phase (the average difference is *ca*. 5%) and at most 30% in the water phase due to the "outlier" value of the PA for the 3-OH group (the average difference is *ca.* 15%). More interestingly, the PM6 results have the same behavior as the DFT ones in the both phases.

The gas phase BDE values of myricetin were also compared to the available DFT ones [57], and show a maximal deviation of 12% with an average deviation of 6%, and the values follow have the same behavior in both cases.

**Table 6** Reaction energies (computed as differences of heats of formation) for the reactions involved in the various mechanisms of antioxidant activity of myricetin (M) in the gas and water phases. IP – ionization potential; PDE – proton dissociation enthalpy; PA – proton affinity; ETE – electron transfer enthalpy; BDE – bond dissociation enthalpy. $\Delta_{ac}H$ – acidity. All values are in kJ mol$^{-1}$. Where available, literature data are included for comparison

| | | IP | PDE | PA | $\Delta_{ac}H^A$ | $\Delta_{ac}H^B$ | $\Delta_{ac}H^C$ | ETE | BDE | BDE$^D$ |
|---|---|---|---|---|---|---|---|---|---|---|
| M(g) | 3 | 790.67 | 877.49 | 1305.54 | 1397.46 | 1425.91 | 1400.80 | 362.62 | 355.98 | 355.64 |
| | 5 | | 965.85 | 1320.51 | 1415.45 | 1455.61 | 1425.91 | 436.02 | 444.34 | 416.73 |
| | 7 | | 947.73 | 1281.79 | 1352.69 | 1396.62 | 1369.42 | 456.62 | 426.22 | 391.20 |
| | 3′ | | 865.68 | 1321.55 | 1352.27 | 1398.71 | 1366.08 | 334.80 | 344.17 | 303.34 |
| | 4′ | | 867.18 | 1318.09 | 1307.50 | 1344.74 | 1317.12 | 339.76 | 345.67 | 308.78 |
| | 5′ | | 877.90 | 1361.37 | 1356.45 | 1401.64 | 1367.75 | 307.20 | 356.39 | 351.46 |
| M (w) | 3 | 624.30 | 1037.01 | 1106.53 | 1415.45 | | | 554.78 | 349.13 | |
| | 5 | | 1118.33 | 1103.59 | 1264.82 | | | 639.04 | 430.44 | |
| | 7 | | 1112.65 | 1101.54 | 1240.97 | | | 635.41 | 424.76 | |
| | 3′ | | 1034.37 | 1115.34 | 1248.51 | | | 543.33 | 346.49 | |
| | 4′ | | 1040.37 | 1123.20 | 1224.24 | | | 541.47 | 352.48 | |
| | 5′ | | 1029.69 | 1124.44 | 1249.34 | | | 529.55 | 341.81 | |

A – acidity data taken from reference 41, obtained with a B3LYP method and a 6-311++G** basis set; B – data taken from reference 56, obtained at the B3LYP/6-31G(d) level; C – data taken from reference 56, obtained at the B3LYP/6-311G(2d,p) level; D – data taken from reference 61, obtained with a ONIOM-G3B3 method.

The gas phase PA values of quercetin (Table 7) were compared to the corresponding acidities, enthalpy changes and Gibbs energy changes [33, 41, 56], and a maximal 10% deviation (with an average 5% deviation) was found between the different sets of values and the PM6 ones; in the water phase the maximal deviation was of 13% and the average deviation of 10%. As before, the data show the same behavior.

The gas phase BDE values also follow the same trends as the published ones [57, 58], with a global average deviation of 13% and a maximal of 45%; however, if we do not consider the ΔG values presented in Table 8, those deviations fall to, respectively, to 10% and 18%; the larger deviations found with the Gibbs energy values are likely to come from differences in the entropic part of the Gibbs energy, which, although expectably small, may contribute to the overall deviations. The water phase BDE values also follow the same trends, with the exception of the PM6 value for the 3-OH BDE which is higher than expected from comparison with the other data, and show an average deviation of 5% with a maximal deviation of 24%. The distribution of the values discussed above is shown in Fig. 4.

## The H atom transfer (HAT) mechanism

The water phase BDE values for quercetin indicate that H atom abstraction occurs primarily from the 3′ and 4′ OH groups, and the resulting radicals are *ca.* 70 kJ mol$^{-1}$ more stable then the following one, from the 7-OH group. In the case of myricetin, H atom abstraction occurs primarily from the B ring OH groups, being the resulting radicals stabilized by the H bonds established with the oxygen atoms in that ring.

These results are in agreement with the established structure-activity relationships for the antioxidant activity of flavones, which point out the fundamental role of the B ring catechol (or pyrogallol) groups [3]. Strikingly, the DFT results suggest that the 3-OH group of quercetin is the one more prone to suffer H atom abstraction in the water phase, in contrast with the gas phase DFT results that point out the 4′ as the one most prone to yield H$^{\bullet}$.

In both flavonoids, the 3-OH H atom is the first one to be abstracted after the B ring H atoms have been removed, explaining experimental results that suggest that the C ring hydroxyl group, when present, potentiates the antioxidant activity that is mainly determined by the B ring OH groups and the C2-C3 double bond [59–62].

## The sequential protol-loss electron-transfer (SPLET) mechanism

The SPLET mechanism is primarily governed by the ease of deprotonation, which can be described by the PA values, and secondarily by the ease of electron transfer from the

**Table 7** Reaction energies (computed as differences of heats of formation) for the reactions involved in the various mechanisms of antioxidant activity of quercetin (Q) in the gas and water phases. IP – ionization potential; PDE – proton dissociation enthalpy; PA – proton affinity; ETE – electron transfer enthalpy; BDE – bond dissociation enthalpy. $\Delta_{ac}H$ – acidity. All values are in kJ mol$^{-1}$. Where available, literature data are included for comparison

| | | IP | PDE | PA | $\Delta_rH$ ($\Delta_rG$)[A] | $\Delta_{ac}H^B$ | $\Delta_{ac}H^C$ | $\Delta_{ac}H^D$ | ETE | BDE | $\Delta_rH$ ($\Delta_rG$)[A] | BDE[E] | BDE[F] |
|---|---|---|---|---|---|---|---|---|---|---|---|---|---|
| Q (g) | 3 | 784.17 (682.41[33]) | 881.41 | 1321.17 | 1385.74 (1387.41) | 1393.69 | 1432.18 | 1410.01 | 344.42 | 353.40 | 322.59 (287.86) | 357.73 | 350.20 (333.46) |
| | 5 | | 973.02 | 1328.71 | 1414.19 (1412.52) | 1411.68 | 1458.96 | 1437.20 | 428.48 | 445.01 | 384.93 (247.27) | 417.98 | 415.47 (396.22) |
| | 7 | | 952.66 | 1288.94 | 1349.76 (1351.01) | 1349.34 | 1392.44 | 1373.19 | 447.90 | 424.65 | 347.27 (311.71) | 389.95 | 370.70 (353.13) |
| | 3′ | | 886.66 | 1375.97 | 1357.29 (1368.17) | 1352.69 | 1398.29 | 1366.49 | 294.86 | 358.65 | 303.34 (269.03) | 342.25 | 322.17 (307.94) |
| | 4′ | | 864.61 | 1293.64 | 1328.42 (1331.35) | 1324.24 | 1359.80 | 1336.37 | 355.14 | 336.60 | 292.88 (259.83) | 329.28 | 312.13 (297.48) |
| Q (w) | 3 | 621.25 (696.66[36]) | 1036.94 | 1118.02 | 1213.78 (1206.25) | 1254.36 | | | 540.17 | 346.01 | 322.59 (276.98) | | |
| | 5 | | 1108.72 | 1130.02 | 1222.98 (1222.56) | 1264.82 | | | 599.96 | 340.65 | 366.94 (330.12) | | |
| | 7 | | 1096.52 | 1096.45 | 1199.55 (1201.65) | 1240.97 | | | 621.32 | 328.45 | 365.68 (323.00) | | |
| | 3′ | | 1036.62 | 1134.68 | 1212.52 (1209.18) | 1248.09 | | | 523.19 | 268.55 | 332.21 (289.53) | | |
| | 4′ | | 1033.15 | 1114.57 | 1197.88 (1194.53) | 1254.78 | | | 539.83 | 265.07 | 319.24 (286.19) | | |

A – data taken from reference [33], obtained with a B3LYP method and a 6-31G* basis set for C and H atoms and a 6-31 + G* basis set for O atoms; B – acidity data taken from reference [41], obtained with a B3LYP method and a 6-311++G** basis set; C – data taken from reference 56, obtained at the B3LYP/6-31G(d) level; D – data taken from reference 56, obtained at the B3LYP/6-311G(2d,p) level; E – data taken from reference 61, obtained with a ONIOM-G3B3 method; F – data taken from reference 62 using the B3P86 and the B3LYP methods with a 6-311 + G(d,p) basis set.

**Table 8** Order of H atom abstraction and deprotonation of hydroxylic H atoms of quercetin (Q) and myricetin (M) in the gas and water phases obtained with the PM6 model. Data from the literature is also included for comparison

| | | Method | Order | Ref. |
|---|---|---|---|---|
| **H atom abstraction** | **Q (g)** | UHF/6-31G* | 3′-4′-3-5-7 | 36 |
| | | AM1 | 3-4′-3′-7-5 | 37 |
| | | B3LYP/6-311++G(3df,2p) | 4′-3′-3-7-5 | 40 |
| | | B3LYP/6-31 + G* | 4′-3′-3-7-5 | 41 |
| | | PM6 | 4′-3-3′-7-5 | a) |
| | **Q (w)** | B3LYP/6-311++G(3df,2p) | 3-4′-3′-… | 40 |
| | | B3LYP/6-31 + G* | 3-4′-3′-7-5 | 41 |
| | | PM6 | 4′-3′-7-5-3 | a) |
| | **M (g)** | PM6 | 3′-4′-3-5′-7-5 | a) |
| | **M (w)** | PM6 | 5′-3′-3-4′-7-5 | a) |
| **Deprotonation** | **Q (g)** | B3LYP/6-311 + G(3df,2p) | 4′-7-3′-3-5 | 39 |
| | | B3LYP/6-311 + G(d,p) | 4′-3′-7-3-5 | 42 |
| | | MP2/6-311++G(d,p) | 4′-7-3-3′-5 | 43 |
| | | B3LYP/6-31 + G* | 4′-7-3′-3-5 | 41 |
| | | PM6 | 7-4′-3-5-3′ | a) |
| | **Q (w)** | B3LYP/6-311++G(3df,2p) | 7-3′-3-4′-5 | 39 |
| | | B3LYP/6-31 + G* | 4′-7-3-3′-5 | 41 |
| | | PM6 | 7-4′-3-5-3′ | a) |
| | **M (g)** | B3LYP/6-311 + G(3df,2p) | 4′-3′-7-5′-3-5 | 39 |
| | | B3LYP/6-311 + G(d,p) | 4′-7-3′-5′-3-5 | 42 |
| | | PM6 | 7-3-4′-5-3′-5′ | a) |
| | **M (w)** | B3LYP/6-311 + G(3df,2p) | 4′-7-3′-5′-3-5 | 39 |
| | | PM6 | 7-5-3-3′-4′-5′ | a) |

a) This work.

anions, described by the ETE. Concerning the deprotonation step, which, as expected, is more favorable in water than in the gas phase, the PA values presented in Tables 6 and 7 indicate that myricetin deprotonates slightly easier than quercetin. For quercetin, the most acidic proton is the 7-OH one, followed by the 4′ one, which is in agreement with the majority of the DFT data available that show that these are two most acidic protons. In the case of myricetin, the PM6 results indicate that the 7-OH proton is also the most acidic one, followed by the 3-OH one in the gas phase and the 5-OH one in the water phase, in clear disagreement with the DFT results indicate that the 4′ is the most acidic one followed by the 7 and 3′ ones. However, the results of Martins et al. [56] indicate that, in solution, flavones deprotonation occurs primarily from the 7-OH group, in agreement with our PM6 data. After deprotonation, the anions may proceed to form the corresponding radicals by electron transfer (measurable by ETE). The ETE values for the flavonoids are in the same order of magnitude, and follow the same trend for both flavonoids.

Considering the set of these results, the SPLET mechanism is expected to be more relevant for myricetin than for quercetin. Moreover, taking into account that the more acidic protons are, in general, the same atoms that are more likely to be abstracted as $H^{\bullet}$, it is expectable that, in aqueous solutions, as are most of the biological environments that surround flavonoids in organisms, the SPLET mechanism will prevail over the HAT one.

## The sequential electron-transfer proton-transfer (SETPT) mechanism

Electron removal from the neutral flavonoids, leading to the formation of the radical cations, is the first step of the SETPT mechanism. As it can be seen from the ionization potentials, this process is slightly more favorable for quercetin than for myricetin.

Contrarily to deprotonation, which occurs spontaneously in water, ionization requires an electron acceptor, thus being more likely to occur in the presence of such acceptors, as are proteins, or, in the case of flavonoid-solvent systems, in the presence of polar solvents, preferentially those able to establish H bonds with the flavonoid molecules, thus further stabilizing the radical cation [21].

The radical cations of both flavonoids undergo a favorable deprotonation in aqueous solution, and the protons involved in these deprotonation are the same mentioned in the above analyzed mechanisms – in myricetin, deprotonation of the radical cation occurs primarily from the central 4′-OH group in the B ring, followed by the neighboring two OH groups, and in quercetin it occurs from the 4′-OH and the 3′-OH groups.

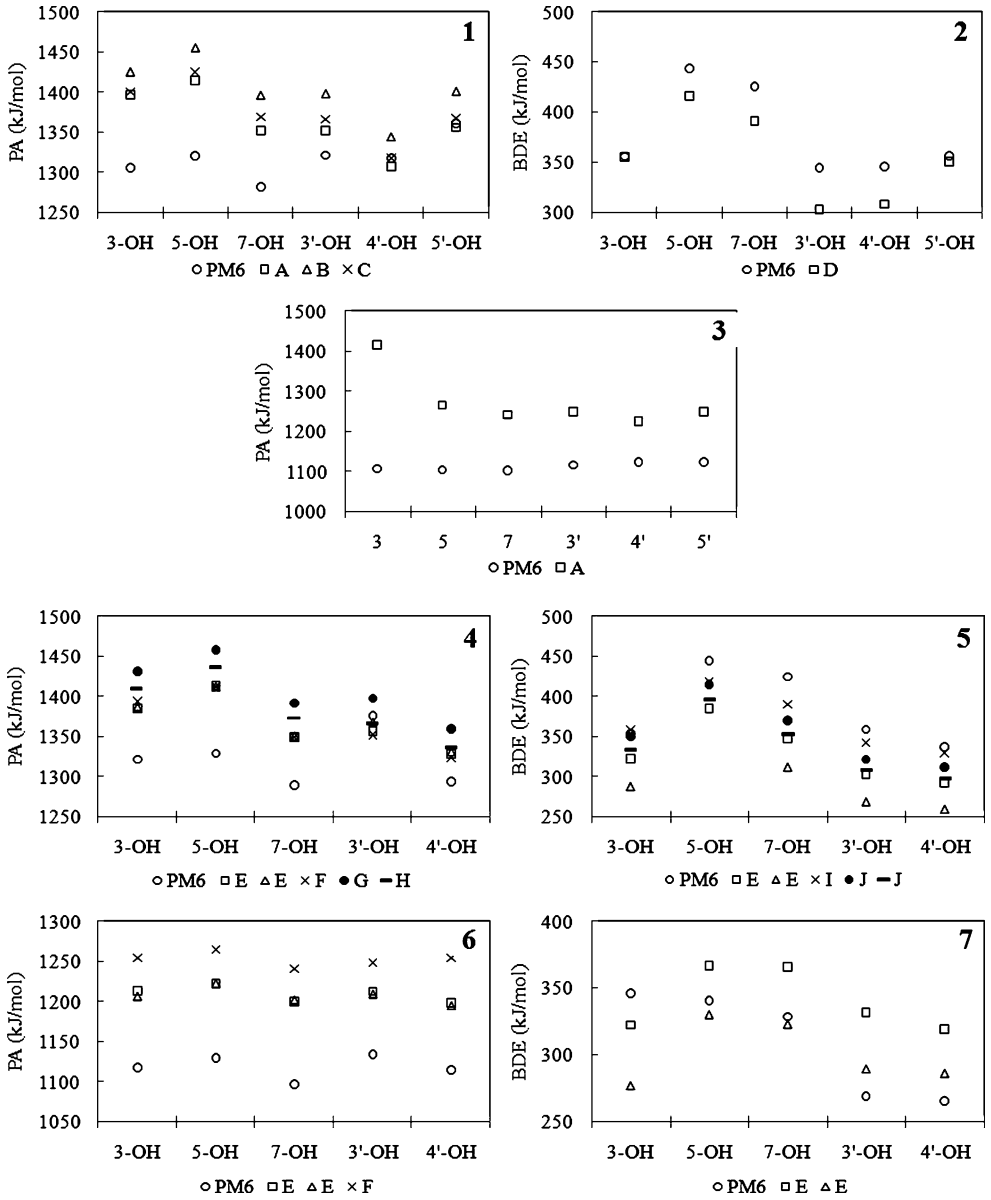


**Fig. 4** Comparison of the proton affinities (PA) and bond dissociation enthalpies (BDE) values of quercetin and myricetin computed with the PM6 method and the corresponding DFT values retrieved from the literature. **1**) PA values of myricetin in the gas phase; **2**) BDE values of myricetin in the gas phase; **3**) PA values of myricetin in the water phase; **4**) PA values of quercetin in the gas phase; **5**) BDE values of quercetin in the gas phase; **6**) PA values of quercetin in the water phase; **7**) BDE values of quercetin in the water phase. Legends: ○PM6: values computed with the PM6 method (this work); **a**: acidity values ($\Delta_{ac}H$) at the B3LYP/6-311++G** level [41]; **b**: acidity values ($\Delta_{ac}H$) at the B3LYP/6-31G(d) level [56]; **C**: acidity values ($\Delta_{ac}H$) at the B3LYP/6-311G(2d,p) level [56]; **d**: BDE values obtained with a ONIOM/G3B3 method [61]; **e**: acidity values (expressed as enthalpy – blank squares – or Gibbs energy – blank triangles - changes) at the B3LYP/6-31G* level for C and H atoms and B3LYP/6-31 + G* level for O atoms [33]; **f**: acidity values ($\Delta_{ac}H$) at the B3LYP/6-311++G** [41]; **g**: acidity values ($\Delta_{ac}H$) at the B3LYP/6-31G(d) [56]; **h**: acidity values ($\Delta_{ac}H$) at the B3LYP/6-311G(2d,p) [56]; **i**: BDE values obtained with a ONIOM/G3B3 method [61]; **j**: BDE values (expressed as enthalpy – circle – or Gibbs energy – rectangle - changes) using the B3P86 and the B3LYP methods with a 6-311 + G (d,p) basis set [62]

## Conclusion

In this work we have reported the results of a semi-empirical study of two flavonoids, quercetin and myricetin. Five different semi-empirical methods were employed, and the results obtained with the PM6 method are, in general, in good agreement with other results published using the density functional theory, thus validating the use of this method to study these compounds.

The PM6 calculations led to nearly planar structures of all the analyzed species, either neutral, radicals or anions, in agreement with results from other authors. Quite noticeably,

the PM6 method is capable of reproducing the charge delocalization and the resonance characteristics of the flavonoids obtained by other authors using a DFT approach. The ionization potentials and the electron affinities computed using the PM6 results, as well as the other computed molecular properties (electronegativity, HOMO-LUMO gap, hardness, electrophilicity and permanent dipole moment) show trends that accompany the ones observed with DFT derived data. However, the PM6 values quite often differ from the DFT ones by more than 50%; nevertheless, those differences became smaller when one uses the energies of the species involved instead of the energies of the orbitals.

The sites of H atom abstraction and the deprotonation orders are also in general agreement with the DFT data. In the case of quercetin, H atom abstraction is expected to occur from the 3′ and 4′ sites, with a possible contribution in the gas phase from the 3-OH group, which are the same three sites predicted to be more important by the DFT results. This is accompanied by the trends in the proton affinities (PA) and bond dissociation enthalpies (BDE), which are in general agreement with the trends observed for the same values obtained with the DFT procedures. Noticeably, the PM6-derived PA values are lower than the DFT ones while the PM6 BDE values are higher than the DFT ones, which indicates that the semi-empirical methods tend to overestimate the energetics of the anions and underestimate the energetic of the radicals when compared with the DFT methods. These results indicate that the semi-empirical PM6 method can be used for, at least, a semi-quantitative approach to the energetic and molecular properties of these compounds.

**Acknowledgments** G. C. J. would like to acknowledge a post-doctoral grant from Fundação para a Ciência e a Tecnologia (SFRH/BPD/2006/27563). The authors would also like to thank Dr. Marta Corvo and one of the reviewers for very significant discussions.

## References

1. Manach C, Scalbert A, Morand C, Rémésy C, Jiménez L (2004) Polyphenols: food sources and bioavailability. Am J Clin Nutr 79:727–747
2. Birt DF, Hendrich S, Wang W (2001) Dietary agents in cancer prevention: flavonoids and isoflavonoids. Pharmacol Ther 90:157–177. doi:10.1016/S0163-7258(01)00137-1
3. Bors W, Michel C (2002) Chemistry of the antioxidant effect of polyphenols. Ann N Y Acad Sci 957:57–69. doi:10.1111/j.1749-6632.2002.tb02905.x
4. Halliwell B, Rafter J, Jenner A (2005) Health promotion by flavonoids, tocopherols, tocotrienols, and other phenols: direct or indirect effects? Antioxidant or not? Am J Clin Nutr 81(1 Suppl): 268S–276S
5. Williamson G, Manach C (2005) Bioavailability and bioefficacy of polyphenols in humans. II. Review of 93 intervention studies. Am J Clin Nutr 81(1 Suppl):243S–255S
6. Gomes A, Fernandes E, Lima JL, Mira L, Corvo ML (2008) Molecular mechanisms of anti-inflammatory activity mediated by flavonoids. Curr Med Chem 15:1586–1605
7. Friedman M (2007) Overview of antibacterial, antitoxin, antiviral, and antifungal activities of tea flavonoids and teas. Mol Nutr Food Res 51:116–134. doi:10.1002/mnfr.200600173
8. Biesalski HK (2007) 9: Polyphenols and inflammation: basic interactions. Curr Opin Clin Nutr Metab Care 10:724–728
9. Wang Y, Yang L, He YQ, Wang CH, Welbeck EW, Bligh SWA, Wang ZT (2008) Characterization of fifty-one flavonoids in a Chinese herbal prescription Longdan Xiegan Decoction by high-performance liquid chromatography coupled to electrospray ionization tandem mass spectrometry and photodiode array detection. Rapid Commun Mass Spectrom 22:1767–1778. doi:10.1002/rcm.3536
10. Heinrich M (2003) Ethnobotany and natural products: the search for new molecules, new treatments of old diseases or a better understanding of indigenous cultures? Curr Top Med Chem 3:29–42
11. Arts IC (2008) A review of the epidemiological evidence on tea, flavonoids, and lung cancer. J Nutr 138:1561S–1566S
12. Tomar RS, Shiao R (2008) Early life and adult exposure to isoflavones and breast cancer risk. J Environ Sci Health C Environ Carcinog Ecotoxicol Rev 26:113–173. doi:10.1080/10590500802074256
13. Linseisen J, Rohrmann S (2008) Biomarkers of dietary intake of flavonoids and phenolic acids for studying diet-cancer relationship in humans. Eur J Nutr 47:60–68. doi:10.1007/s00394-008-2007-x
14. de Kok TM, van Breda SG, Manson MM (2008) Mechanisms of combined action of different chemopreventive dietary compounds: a review. Eur J Nutr 47(Suppl 2):51–59. doi:10.1007/s00394-008-2006-y
15. Manach C, Williamson G, Morand C, Scalbert A, Rémésy C (2005) Bioavailability and bioefficacy of polyphenols in humans. I. Review of 97 bioavailability studies. Am J Clin Nutr 81(1 Suppl): 230S–242S
16. Boots AW, Haenen GR, Bast A (2008) Health effects of quercetin: from antioxidant to nutraceutical. Eur J Pharmacol 585:325–327. doi:10.1016/j.ejphar.2008.03.008
17. Oyama Y, Fuchs PA, Katayama N, Noda K (1994) Myricetin and quercetin, the flavonoid constituents of Ginkgo biloba extract, greatly reduce oxidative metabolism in both resting and Ca(2+)-loaded brain neurons. Brain Res 635:125–129. doi:10.1016/0006-8993(94)91431-1
18. Gordon MH, Roedig-Penmanm A (1998) Antioxidant activity of quercetin and myricetin in liposomes. Chem Phys Lipids 97:79–85. doi:10.1016/S0009-3084(98)00098-X
19. Furuno K, Akasako T, Sugihara N (2002) The contribution of the pyrogallol moiety to the superoxide radical scavenging activity of flavonoids. Biol Pharm Bull 25:19–23. doi:10.1248/bpb.25.19
20. Zhang H-Y, Sun Y-M, Wang X-L (2003) Substituent effects on O-H bond dissociation enthalpies and ionization potentials of catechols: A DFT study and its implications in the rational design of phenolic antioxidants and elucidation of structure-activity relationships for flavonoid antioxidants. Chem Eur J 9:502–508. doi:10.1002/chem.200390052
21. Litwinienko G, Ingold KU (2007) Solvent effects on the rates and mechanisms of reaction of phenols with free radicals. Acc Chem Res 40:222–230. doi:10.1021/ar0682029
22. Mayo SL, Olafson BD, Goddard WA III (1990) DREIDING: a generic force field for molecular simulations. J Phys Chem 94:8897–8909. doi:10.1021/j100389a010

23. Marvin version 5.00 and Calculator Plugins for Marvin 500 2008 ChemAxon (http://wwwchemaxoncom)
24. MOPAC2009 James J P Stewart Stewart Computational Chemistry Version 9034 L. http://OpenMOPACnet
25. Baker J (1986) An algorithm for the location of transition states. J Comp Chem 7:385–395. doi:10.1002/jcc.540070402
26. Dewar MJS, Thiel W (1977) Ground states of molecules. 38. The MNDO method. Approximations and parameters. J Am Chem Soc 99:4899–4907. doi:10.1021/ja00457a004
27. Dewar MJS, Zoebisch EG, Healy EF, Stewart JJP (1985) Development and use of quantum mechanical molecular models. 76. AM1: a new general purpose quantum mechanical molecular model. J Am Chem Soc 107:3902–3909. doi:10.1021/ja00299a024
28. Rocha GB, Freire RO, Simas AM, Stewart JJP (2006) RM1: A reparameterization of AM1 for H, C, N, O, P, S, F, Cl, Br, and I. J Comp Chem 27:1101–1111. doi:10.1002/jcc.20425
29. Stewart JJP (1989) Optimization of parameters for semiempirical methods I. Method J Comp Chem 10:209–220. doi:10.1002/jcc.540100208
30. Stewart JJP (2007) Optimization of parameters for semiempirical methods V: modification of NDDO approximations and application to 70 elements. J Mol Modeling 13:1173–1213. doi:10.1007/s00894-007-0233-4
31. Klamt A, Schüürmann G (1993) COSMO: a new approach to dielectric screening in solvents with explicit expressions for the screening energy and its gradient. J Chem Soc Perkin Trans 2:799–805. doi:10.1039/P29930000799
32. Antonczak S (2008) Electronic description of four flavonoids revisited by DFT method. THEOCHEM 856:38–45. doi:10.1016/j.theochem.2008.01.014
33. Fiorucci S, Golebiowski J, Cabrol-Bass D, Antonczak S (2007) DFT study of quercetin activated forms involved in antiradical, antioxidant, and prooxidant biological processes. J Agric Food Chem 55:903–911. doi:10.1021/jf061864s
34. Klein E, Lukeš V, Ilčin M (2007) DFT/B3LYP study of tocopherols and chromans antioxidant action energetics. Chem Phys 336:51–57. doi:10.1016/j.chemphys.2007.05.007
35. Lide DA (2004) CRC handbook chemistry and physics. CRC Press Inc, Boca Raton, FL, USA
36. Parr RG, Szentpály L, Liu S (1999) Electrophilicity index. J Am Chem Soc 121:1922–1924. doi:10.1021/ja983494x
37. Mendoza-Wilson AM, Glossman-Mitnik D (2005) CHIH-DFT study of the electronic properties and chemical reactivity of quercetin. THEOCHEM 716:67–72. doi:10.1016/j.theochem.2004.10.083
38. Vasilescu D, Girma R (2002) Quantum molecular modeling of quercetin - simulation of the interaction with the free radical t-BuOO. Int J Quantum Chem 90:888–902. doi:10.1002/qua.1801
39. Russo N, Toscano M, Occella N (2000) Semiempirical molecular modeling into quercetin reactive site: structural, conformational, and electronic features. J Agric Food Chem 48:3232–3237. doi:10.1021/jf990469h
40. Leopoldini M, Marino T, Russo N, Toscano M (2004) Antioxidant Properties of Phenolic Compounds: H-Atom versus Electron Transfer Mechanism. J Phys Chem A 108:4916–4922. doi:10.1021/jp037247d
41. Leopoldini M, Russo N, Toscano M (2006) Gas and liquid phase acidity of natural antioxidants. J Agric Food Chem 54:3078–3085. doi:10.1021/jf053180a
42. Leopoldini M, Marino T, Russo N, Toscano M (2004) Density functional computations of the energetic and spectroscopic parameters of quercetin and its radicals in the gas phase and in solvent. Theor Chem Acc 111:210–216. doi:10.1007/s00214-003-0544-1
43. Carpenter JE, Weinhold F (1988) Analysis of the geometry of the hydroxymethyl radical by the "different hybrids for different spins" natural bond orbital procedure. THEOCHEM 169:41–62. doi:10.1016/0166-1280(88)80248-3
44. Carpenter JE, Reed WF, AE WF (1985) Natural localized molecular orbitals. J Chem Phys 83:1736–1740. doi:10.1063/1.449360
45. Cornard JP, Merlin JC, Boudet AC, Vrielynck L (1997) Structural study of quercetin by vibrational and electronic spectroscopies combined with semiempirical calculations. Biospectroscopy 3:183–193. doi:10.1002/(SICI)1520-6343(1997)3:3<183::AID-BSPY2>3.0.CO;2-7
46. van Acker SABE, de Groot MJ, van den Berg M-J, Tromp MNJL, den Kelder GD-O, Vijgh WJF, Bast A (1996) A quantum chemical explanation of the antioxidant activity of flavonoids. Chem Res Toxicol 9:1305–1312. doi:10.1021/tx9600964
47. Yates PC (1991) Semi-empirical molecular orbital calculations on tyrosine kinase inhibitors and structurally related compounds. THEOCHEM 231:201–213. doi:10.1016/0166-1280(91)85 218-V
48. Erlejman AG, Verstraeten SV, Fraga CG, Oteiza PI (2004) The interaction of flavonoids with membranes: potential determinant of flavonoid antioxidant effects. Free Radic Res 38:1311–1320. doi:10.1080/10715760400016105
49. Olivero-Verbel J, Pacheco-Londoño L (2002) Structure−Activity Relationships for The Anti-HIV Activity of Flavonoids. J Chem Inf Comput Sci 42:1241–1246. doi:10.1021/ci020363d
50. Bonin KD, Kresin VV (1997) Electric-Dipole Polarizabilities of Atoms Molecules and Clusters. World Scientific, Singapore
51. Foresman JB, Frisch AE (1996) Exploring Chemistry with Electronic Structure Methods. Gaussian, Pittsburgh PA, USA
52. Lewars E (2003) Computational Chemistry—Introduction to the Theory and Applications of Molecular and Quantum Mechanics. Kluwer Academic Publishers, Norwell MA, USA
53. Hatch FT, Lightstone FC, Colvein ME (2000) Quantitative structure-activity relationship of flavonoids for inhibition of heterocyclic amine mutagenicity. Environ Mol Mutagen 35:279–299. doi:10.1002/1098-2280(2000)35:4<279::AID-EM3>3.0.CO;2-9
54. Rasulev BF, Abdullaev ND, Syrov VN, Leszczynski J (2005) A quantitative structure-activity relationship (QSAR) study of the antioxidant activity of flavonoids. QSAR Combin. Sci 24:1056–1065. doi:10.1002/qsar.200430013
55. Chaudière J, Ferrari-Iliou R (1999) Intracellular antioxidants: from chemical to biochemical mechanisms. Food Chem Toxicol 37:949–962. doi:10.1016/S0278-6915(99)00090-3
56. Martins HFP, Fernandez MT, Lopes VHC, Cordeiro MNDS (2004) Toward the prediction of the activity of antioxidants: experimental and theoretical study of the gas-phase acidities of flavonoids. J Am Soc Mass Spectrom 15:848–861. doi:10.1016/j.jasms.2004.02.007
57. Li MJ, Liu L, Fu Y, Guo QX (2007) Accurate bond dissociation enthalpies of popular antioxidants predicted by the ONIOM-G3B3 method. THEOCHEM 815:1–9. doi:10.1016/j.theochem.2007.03.012
58. Trouillas P, Marsal P, Siri D, Lazzaroni R, Duroux JL (2006) A DFT study of the reactivity of OH groups in quercetin and taxifolin antioxidants: the specificity of the 3-OH site. Food Chem 97:679–688. doi:10.1016/j.foodchem.2005.05.042
59. Wolfe KL, Liu RH (2008) Structure−activity relationships of flavonoids in the cellular antioxidant activity assay. J Agric Food Chem 56:8404–8411. doi:10.1021/jf8013074
60. Munoz-Munoz JL, Garcia-Molina F, Molina-Alarcón M, Tudela J, Carcía-Cánovas F, Rodríguez-López JN (2008) Kinetic character-

ization of the enzymatic and chemical oxidation of the catechins in green tea. J Agric Food Chem 56:9215–9224. doi:10.1021/jf8012162

61. Tsimogiannis DI, Oreopoulou V (2005) The contribution of flavonoid C-ring on the DPPH free radical scavenging efficiency. A kinetic approach for the 3′,4′-hydroxy substituted members. Innov Food Sci Emerg Technol 7:140–146. doi:10.1016/j.ifset.2005.09.001
62. Wang LF, Zhang HY (2004) Unexpected role of 5-OH in DPPH radical-scavenging activity of 4-thiaflavans. Revealed by theoretical calculations. Bioorg Med Chem Lett 14:2609–2611. doi:10.1016/j.bmcl.2004.02.066